Carrier statistics and quantum capacitance of graphene sheets and ribbons

Tian Fang, Aniruddha Konar, Huili Xing, and Debdeep Jena[a)]
Department of Electrical Engineering, University of Notre Dame, Indiana, 46556

In this work, fundamental results for carrier statistics in graphene two-dimensional sheets and nanoscale ribbons are derived. Though the behavior of intrinsic carrier densities in two-dimennsional graphene sheets is found to differ drastically from traditional semiconductors, very narrow (sub-10 nm) ribbons are found to be similar to traditional narrow-gap semiconductors. The quantum capacitance, an important parameter in the electrostatic design of devices, is derived for both two-dimensional graphene sheets and nanoribbons. © *2007 American Institute of Physics.* [DOI: 10.1063/1.2776887]

Graphene, a two-dimensional (2D) honeycomb structure of carbon atoms, has generated intense interest recently.[1–5] It has been now demonstrated that narrow graphene nanoscale ribbons (GNRs) possess band gaps that are tuned by the ribbon width.[3] These properties, along with the good transport properties of carriers (high mobility, high Fermi velocity) suggest that it is possible that graphene may be used in the near future in high speed electronic devices.[6,7] In spite of rapid advances in the study of transport properties of graphene, basic tools of semiconductor device design such as temperature dependent carrier statistics and electrostatic properties such as quantum capacitance remain unexplored. This work investigates these properties for both 2D sheets, and GNRs in a comparative fashion, and analytical results for these quantities are presented.

The dispersion of mobile π electrons in graphene in the first Brillouin zone (BZ) is given by

$$E(\mathbf{k}) = s\hbar v_F |\mathbf{k}|, \tag{1}$$

where $s=+1$ is the conduction band (CB) and $s=-1$ is the valence band (VB), $\hbar$ is the reduced Planck's constant, $v_F \sim 10^8$ cm/s is the Fermi velocity of carriers in graphene, and $|\mathbf{k}| = \sqrt{k_x^2 + k_y^2}$ is the wave vector of carriers in the 2D $(x-y)$ plane of the graphene sheet. The point $|\mathbf{k}|=0$, referred to as the "Dirac point," is a convenient choice for the reference of energy; thus, $E(|\mathbf{k}|=0)=0$ eV. Each $\mathbf{k}$ point is twofold spin degenerate ($g_s=2$), and there are two valleys in the first BZ (the K and K' valleys), $g_v=2$. Deviations from the conical bandstructure are neglected in this work.

In an undoped layer of graphene in thermal equilibrium, there are mobile electrons in the CB and holes in the VB, similar to the intrinsic carriers in a pure bulk semiconductor. To find the 2D sheet density of such intrinsic carriers in graphene, the linear density of states (DOS),

$$\rho_{gr}(E) = \frac{g_s g_v}{2\pi(\hbar v_F)^2} |E|, \tag{2}$$

is used to write the 2D electron gas sheet density in graphene as

$$n = \int_0^\infty dE \rho_{gr}(E) f(E), \tag{3}$$

where $f(E)$ is the Fermi-Dirac distribution function given by $f(E) = (1+\exp[(E-E_F)/kT])^{-1}$, k the Boltzmann constant, T the absolute temperature, and E_F the Fermi level. With the aid of the dimensionless variables $u=E/kT$ and $\eta=E_F/kT$, the electron density may be rewritten as

$$n = \frac{2}{\pi}\left(\frac{kT}{\hbar v_F}\right)^2 \mathfrak{I}_1(+\eta), \tag{4}$$

and the hole density is symmetric, given by

$$p = \frac{2}{\pi}\left(\frac{kT}{\hbar v_F}\right)^2 \mathfrak{I}_1(-\eta), \tag{5}$$

where $\mathfrak{I}_j(\eta) = 1/\Gamma(j+1)\int_0^\infty du\, u^j/(1+e^{u-\eta})$ is the Fermi-Dirac integral with $j=1$ and $\Gamma(\cdots)$ is the gamma function.

Under thermal equilibrium and under no external perturbation (no applied bias, no optical illumination), the Fermi level is unique, and moreover, it is exactly at the Dirac point ($E_F=0$ eV). Then, the intrinsic carrier concentration in 2D graphene is given by

$$n = p = n_i = \frac{\pi}{6}\left(\frac{kT}{\hbar v_F}\right)^2, \tag{6}$$

which is dependent on only one material parameter—the Fermi velocity. The point to note is that the intrinsic sheet density of electrons/holes does not depend on temperature exponentially; it has a T^2 dependence, due to the absence of a band gap, and the linear energy dispersion. At room temperature, the intrinsic electron and hole sheet densities evaluate to $n_i \sim 9 \times 10^{10}$ cm^{-2}.

The situation changes for nanoscale ribbons cut from infinite graphene sheets. Consider a GNR of width W. Current experimental evidence suggests no clear dependence of the band gap of GNRs on the chirality.[3] Regardless, the results derived here remain applicable for GNRs with band gaps. We make the assumption that the electron and hole quasimomenta are isotropic in the graphene plane. By aligning the x axis along the longitudinal direction of the ribbon, the electron wave vector in the y direction is quantized by hard-wall boundary conditions to be $k_y=n\pi/W$ ($n=\pm 1, \pm 2, \dots$), and the energy dispersion relation [Eq. (1)] for the nth subband becomes

[a)]Electronic mail: djena@nd.edu

$$E(n,k_x) = s\hbar v_F \sqrt{k_x^2 + \left(\frac{n\pi}{W}\right)^2}, \qquad (7)$$

indicating that the CB ($s=1$) and VB ($s=-1$) split into a number of one-dimensional (1D) subbands, indexed by n. It is obvious that breaking the symmetry of a graphene sheet by cutting out a ribbon opens up a band gap. For the isotropic case assumed here, the band gap for a GNR of width W is given by $E_g = E_{s=+1}(1,0) - E_{s=-1}(1,0) = 2\pi\hbar v_F/W$, dependent only on the Fermi velocity and the width of the GNR. The DOS relation for the nth 1D subband is then given by

$$\rho_{GNR}(n,E) = \frac{4}{\pi\hbar v_F}\frac{E}{\sqrt{E^2 - E_n^2}}\Theta(E - E_n), \qquad (8)$$

where $\Theta(\cdots)$ is the Heaviside unit step function and $E_n = n\pi\hbar v_F/W = nE_g/2$. This directly leads to a *total* DOS $\rho_{GNR}(E) = \Sigma_n\rho_{GNR}(n,E)$. The expression for the total DOS is the same for the CB and VB and exhibits Van Hove singularities at energies E_n from the Dirac point. The electron density as a result is given by

$$n = \frac{4kT}{\pi\hbar v_F}\sum_{n>0} S(x_n, \eta), \qquad (9)$$

where $x_n = E_n/kT$, $\eta = E_F/kT$, and

$$S(x, \eta) = \int_x^\infty \frac{u}{\sqrt{u^2 - x^2}}\frac{du}{1 + e^{u-\eta}}. \qquad (10)$$

The intrinsic carrier concentration in GNRs is obtained when $\eta = E_F = 0$, i.e., the Fermi level is at midgap; this leads to $n_i = (4kT/\pi\hbar v_F)\Sigma_n S(x_n,0)$. For narrow GNRs, $E_g \gg kT$, then one can use the approximation $S(x,0) \approx xK_1(x)$ where $K_1(\cdots)$ is the Bessel function of first order, and the asymptotic approximation of the Bessel function $K_1(x) \approx \sqrt{\pi/2x}\exp(-x)$ for large x to write the intrinsic carrier density of GNRs as

$$n_i \approx \frac{4}{W}\sqrt{\frac{\pi kT}{E_g}}\sum_n \sqrt{n}e^{-n(E_g/2kT)}. \qquad (11)$$

For band gaps well in excess of the thermal energy, it suffices to retain only the first term in the summation to recover the familiar dependence,

$$n_i \approx \frac{4}{W}\sqrt{\frac{\pi kT}{E_g}}e^{-E_g/2kT}. \qquad (12)$$

This relation has to be used with caution when experimentally extracting band gaps from the slope of Arrhenius-like plots; it is applicable *only* when the band gap is well in excess of the thermal energy, as has been done in a recent report.[8] The 1D carrier concentration of GNRs may be converted to an effective 2D sheet density by writing $n_{2D} = n_{1D}/W$ for comparing their properties with graphene, as is done in Fig. 1. This figure shows that the intrinsic carrier concentrations in GNRs differs significantly from graphene only if the ribbon widths are below ~ 0.1 μm, and indicates when Arrhenius dependence of intrinsic carrier concentrations is valid.

The carrier sheet density in graphene can be changed by an electrostatic gate voltage, and the on-state sheet densities can approach, and exceed those in conventional field-effect transistors. If the Fermi level in a 2D graphene sheet is
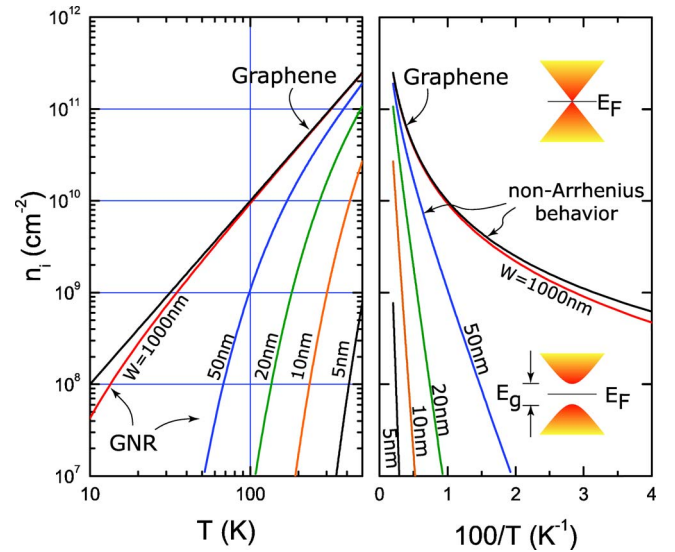

FIG. 1. (Color online) Intrinsic sheet carrier concentrations in graphene sheets and nanoribbons. Wide GNRs and 2D graphene have non-Arrhenius dependence on temperature, which becomes increasingly Arrhenius-like as the ribbon width decreases.

driven from the Dirac point to $E_F = \eta kT$ electrostatically by means of a gate voltage, then the electron density is given by $n = n_i\mathfrak{I}_1(\eta)/\mathfrak{I}_1(0)$ and the hole density by $p = n_i\mathfrak{I}_1(-\eta)/\mathfrak{I}_1(0)$, leading to a mass-action law $np = n_i^2\mathfrak{I}_1(\eta)\mathfrak{I}_1(-\eta)/\mathfrak{I}_1^2(0)$.

Similarly, if the local electrostatic potential in a GNR is tuned by a gate voltage such that the Fermi level is at $E_F = \eta kT$, then the electron density is given by Eq. (9). For $\eta > x \gg 1$, one can make the approximation $[1 + \exp(u-\eta)]^{-1} \approx \Theta(\eta-u)$ to rewrite the 1D electron concentration as

$$n \approx \frac{4}{\pi\hbar v_F}\sum_n \sqrt{E_F^2 - E_n^2}\,\Theta(E_F - E_n), \qquad (13)$$

On the other hand, for a nondegenerate condition when the Fermi level is located inside the GNR band gap, using the approximation $S(x,\eta) \approx \sqrt{\pi x/2}\exp(\eta-x)$ the electron concentration may be written as $n \approx n_i e^\eta$, and similarly, for holes, $p \approx n_i e^{-\eta}$, which is similar to traditional semiconductors. Figure 2 shows the calculated exact 2D carrier concentrations in graphene and GNRs of different widths as a function of the location of the Fermi level ($qV_{ch} = E_F$) at room temperature. Though narrow GNRs exhibit large charge modulation due to the existence of a gap, they become similar to 2D graphene sheets when the Fermi level is deep inside the bands. Ripples appear in the GNR density due to Van Hove singularities, as indicated by arrows.

An important quantity in the design of nanoscale devices is the quantum capacitance.[9] Writing the total charge in a graphene sheet with a local channel electrostatic potential V_{ch} as $Q = q(p-n)$ where q is the electron charge, and using the definition of quantum capacitance $C_Q = \partial Q/\partial V_{ch}$, one obtains for 2D graphene,

$$C_Q = \frac{2q^2 kT}{\pi(\hbar v_F)^2}\ln\left[2\left(1 + \cosh\frac{qV_{ch}}{kT}\right)\right], \qquad (14)$$

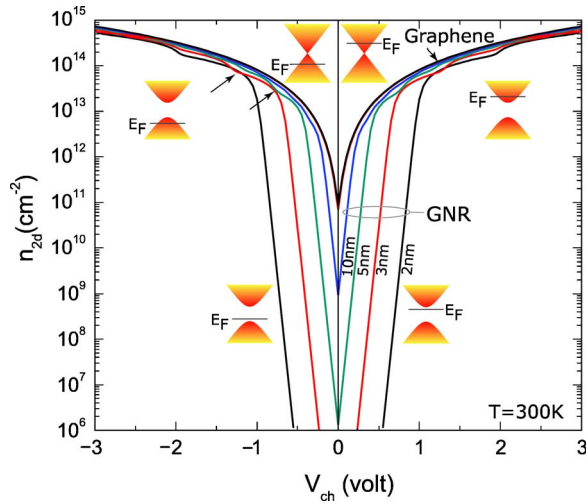which under the condition $qV_{ch} \gg kT$ reduces to

FIG. 2. (Color online) 2D carrier concentration in graphene and GNRs of different widths as a function of the location of the Fermi level. Though narrow GNRs exhibit large charge modulation due to the existence of a gap, they become similar to 2D graphene sheets when the Fermi level is deep inside the bands.

FIG. 3. (Color online) Left: quantum capacitance of 2D graphene and a 5 nm GNR compared with the parallel-plate capacitance of 1 nm SiO$_2$ and HfO$_2$. Right: 2D carrier density in a graphene sheet as a function of gate voltage for different oxide thicknesses.

$$C_Q \approx q^2 \frac{2}{\pi} \frac{qV_{\mathrm{ch}}}{(\hbar v_F)^2} = q^2 \rho_{\mathrm{gr}}(qV_{\mathrm{ch}}). \qquad (15)$$

If the electrostatic capacitance formed between a gate electrode and the graphene layer is given by $C_{\mathrm{ox}} = \epsilon_{\mathrm{ox}}/t_{\mathrm{ox}}$, then the electron density in the graphene layer can be written as a function of the gate voltage as

$$n = n_G - n_Q \left(\sqrt{1 + 2\frac{n_G}{n_Q}} - 1 \right), \qquad (16)$$

where $n_G = C_{\mathrm{ox}} V_G / q$ is the traditional carrier density one would obtain by neglecting the quantum capacitance and $n_Q = (\pi/2)(C_{\mathrm{ox}} \hbar v_F / q^2)^2$, which arises solely due to the quantum capacitance. Applying the same method to find the quantum capacitance (per unit width) of GNRs, one obtains for the condition $\eta > x \gg 1$,

$$C_Q \approx \frac{4q^2}{\pi \hbar v_F} \sum_n \frac{\eta}{\sqrt{\eta^2 - x_n^2}} \Theta(\eta - x_n) = q^2 \rho_{\mathrm{GNR}}(\eta). \qquad (17)$$

The quantum capacitance of 2D graphene and GNR is plotted in Fig. 3 (left), and compared with the oxide gate capacitance of 1 nm SiO$_2$ and HfO$_2$. Figure 3 (right) shows the carrier density dependence in 2D graphene on the gate voltage [Eq. (16)] for different SiO$_2$ thicknesses. Gate modulation of the charge is strong but nonlinear for very thin t_{ox}
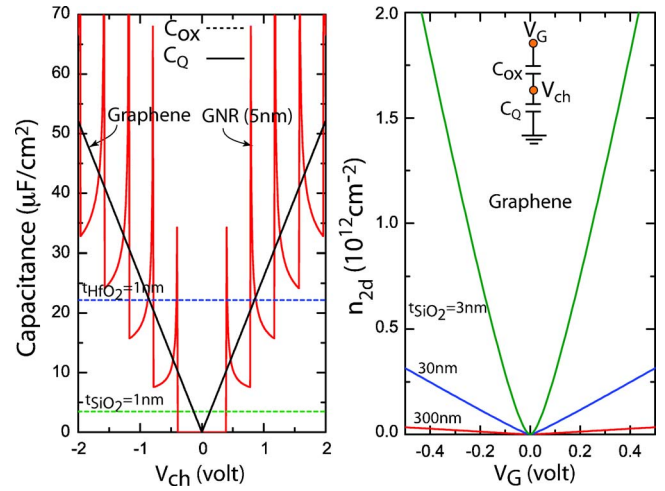
since $C_Q \approx C_{\mathrm{ox}}$ under that condition. The field-effect becomes weak but increasingly linear as t_{ox} is increased since $C_{\mathrm{ox}} \ll C_Q$ under that condition. Thus, by measuring the quantum capacitance, one can directly infer the band gap from the separation of the van Hove singularities. The results presented here would prove useful for the design of electronic devices using graphene sheets and GNRs.

[1] A. K. Geim and K. S. Novoselov, Nat. Mater. **6**, 183 (2007).
[2] K. S. Novoselov, A. K. Geim, S. V. Morozov, D. Jiang, M. I. Katsnelson, I. V. Grigoreva, S. V. Dubonos, and A. A. Firsov, Nature (London) **438**, 197 (2005).
[3] M. Han, B. Ozyilmaz, Yuanbo Zhang, and P. Kim, Phys. Rev. Lett. **98**, 206805 (2007).
[4] C. Berger, Z. Song, X. Li, X. Wu, N. Brown, C. Naud, D. Mayou, T. Li, J. Hass, A. N. Marchenkov, E. H. Conrad, P. N. First, and W. A. de Heer, Science **312**, 1191 (2006).
[5] J.-C. Charlier, X. Blase, and S. Roche, Rev. Mod. Phys. **79**, 677 (2007).
[6] B. Obradovic, R. Kotlyar, F. Heinz, P. Matagne, T. Rakshit, M. D. Giles, M. A. Stettler, and D. E. Nikonov, Appl. Phys. Lett. **88**, 142102 (2006).
[7] M. C. Lemme, T. J. Echtermeyer, M. Baus, and H. Kurz, IEEE Electron Device Lett. **28**, 282 (2007).
[8] Z. Chen, Y.-M. Lin, M. J. Rooks, and P. Avouris, e-print arXiv:cond-mat/0701599.
[9] D. L. John, L. C. Castro, and D. L. Pulfrey, J. Appl. Phys. **96**, 5180 (2004).